J Therm Anal Calorim (2012) 110:523–527
DOI 10.1007/s10973-012-2553-6

Structural and thermal properties of chemically synthesized Bi_2Te_3 nanoparticles

Punita Srivastava · Kedar Singh

SATAC-ACT2011 Conference Special Chapter
© Akadémiai Kiadó, Budapest, Hungary 2012

Abstract Bi_2Te_3 nanoparticles (NPs) have been synthesized at 50 °C by a low-cost wet chemical route. The structural properties of product sample were characterized by powder X-ray diffraction (XRD), transmission electron microscopy (TEM), and scanning electron microscopy. Thermal properties of product sample were investigated by differential scanning calorimetry (DSC), thermogravimetric (TG), and transient plane source techniques. The XRD and selected area electron diffraction of Bi_2Te_3 NPs result showed the polycrystalline nature with a rhombohedral ($R3m$) structure of the nanocrystallites. The average grain size of Bi_2Te_3 NPs was found to be about 30 nm by XRD and TEM measurements. DSC result shows one endothermic peak and one exothermic peak. TG result shows that only 48 % mass loss has occurred in Bi_2Te_3 sample. The obtained lower thermal conductivity of Bi_2Te_3 NPs is about 0.3 W m^{-1} K^{-1} at room temperature, which is caused by considering the crystalline nature of this material.

Keywords Nanoparticles · Chemical synthesis · Electron microscopy · Thermal properties

Introduction

During the last few decades, with the rapid improvement of human society, the consumption of traditional energy has increased exponentially. Thermoelectric (TE) devices emerge as a new type of hot substance that can directly achieve the conversion between heat and electricity, which can maximize the use of waste heat and electricity for present and future. Bismuth telluride and its alloys are recently known as the best TE materials for solid-state cooling devices at room temperature. The energy conversion efficiency mainly depends on the material's dimensionless thermoelectric figure-of-merit $(ZT) = \sigma S^2 T/\kappa$, where σ is the electrical conductivity, S is the Seebeck coefficient; T is the operating temperature, and κ is the thermal conductivity. The quantity $S^2\sigma$ is commonly considered as "power factor." Increment in power factor and decrement in thermal conductivity are essential requirements for the enhancement of ZT value. Reducing the dimensionality and size of the building blocks of TE materials is an efficient and promising way to improve ZT. For example, 1-D quantum rods or 2-D quantum wells of Bi_2Te_3 with a diameter or well width of 5 A may attain the $ZT = 14$ or 5 by theoretical calculations, and Bi_2Te_3/Sb_2Te_3 nanolayer superlattice films at room temperature, Bi_2Te_3/Sb_2Te_3 bulk nanocomposites at 450 K, and nanostructured bismuth antimony telluride bulk alloys at 373 K have been attained the ZT values = 2.4, 1.47, and 1.4 respectively [1–10]. However, solvothermal or hydrothermal reaction process usually requires high pressure and electrodepositing method requires expensive template with special construction on which the product structure strongly depends. Microwave-assisted route is expensive and handled carefully. Thus, for a special purpose to develop a more convenient and rapid way for synthesizing Bi_2Te_3 nanoparticles (NPs) is required. Therefore, low-cost and less hazardous wet-chemical route has been used to synthesize some nanostructures (films, nanorods, nanowires, and nanobelts) of oxides, metals, semimetal, alloys, and other compounds [11–13]. Bi_2Te_3 NPs were successfully synthesized via a wet chemical route in this work.

P. Srivastava · K. Singh (✉)
Department of Physics, Faculty of Science, Banaras Hindu University, Varanasi 221005, India
e-mail: kedarbhp@rediffmail.com

In our recent research work, synthesis of Bi_2Te_3 NPs with diameter about 30 nm has been reported by a facile, one-step, low-cost, and less hazardous wet chemical route at 50 °C. Thermal analysis techniques such as thermogravimetric (TG) and differential scanning calorimetry (DSC) were used for the obtaining process data from the NPs thermal degradation. Transient plane source (TPS) technique is also used to measure the thermal conductivity of as synthesized Bi_2Te_3 NPs.

Materials and methods

In the typical synthesis of Bi_2Te_3 NPs, highly pure tellurium (99.999 %) and Bismuth chloride ($BiCl_3$) purchased from Alfa were used without further purification. Ethylene glycol and hydrazine hydrate (analytical grade) purchased from Merck, Germany, were used as received. In the synthesis, (12 g) bismuth chloride and (6 g) tellurium (in powder form) were taken with deionized water, ethylene glycol, and hydrazine hydrate in a volume ratio of 7:3:1, respectively, in a 200-mL capacity conical flask. Then, the solution was refluxed under vigorous stirring at 50 °C for 5 h. Finally, the black precipitates were collected and washed with anhydrous ethanol and hot distilled water several times and then dried in vacuum at 50 °C for 4 h.

Methods of analysis

The X-ray diffraction (XRD) pattern of the as-synthesized, freshly dried Bi_2Te_3 was recorded using Rigaku Rotoflux rotating anode diffractometer (operating at 40 kV, 100 mA) with Cu-K_α radiation (wavelength 1.54 Å). For microstructural and structural characterization, scanning electron microscopy (SEM) was used to investigate the size and morphology, which was carried out on a scanning electron micro-analyzer using a JEOL JSM6700 microscope operating at 10 A and 20 kV. Transmission electron microscopy (TEM) and high resolution transmission electron microscopy (HRTEM) investigations were carried out using a Tecnai $20G^2$-TEM employing 200 kV typical e-beam voltage using JEOL-JSM-5600. DSC measurements were recorded using a Shimadzu DSC-60 model. Five to ten milligrams (approximate) samples were taken in standard aluminum (Al) pan and scanned over a temperature range from ambient to 502 °C at 10 °C min^{-1} heating rate. TG measurements were analyzed using a Netzsch instrument in nitrogen atmosphere. Samples were heated from ambient to 700 °C at 10 °C min^{-1}. Thermal conductivity measurements were done by transient plane source (TPS-2500) technique.

Results and discussion

Room temperature powder XRD pattern of Bi_2Te_3 sample is shown in Fig. 1. It is believed that the large flexibility of bismuth tellurides in terms of their chemical composition leads to the broad XRD reflections. The XRD pattern in Fig. 1 indicates that the as-synthesized powder has a single phase rhombohedral lattice structure of Bi_2Te_3 (space group of $R\bar{3}m$). The XRD pattern of Bi_2Te_3 sample with characteristic features corresponding to (015), (018), (1010), (0111), (110), (1013), (0114), (0210), (1115), (0021), (1118)s and (2110) planes are in very good agreement with rhombohedral ($R3m$) structure (Joint Committee on Powder Diffraction Standards), JCPDS card No. 08-0021 ($a = 4.384$ Å and $c = 30.45$ Å). The peaks (015) and (1010) are ultra strong as compared to the other peaks. These two diffraction peaks expected for isotropically distributed crystallites, indicate a highly preferential orientation of the NPs along the (015) and (1010) directions, respectively. As expected, the XRD peaks of Bi_2Te_3 were considerably broadened compared to bulk material due to the small size of the NPs. The size of the nanocrystallites were estimated by the Debye–Scherrer formula

$$A = \frac{0.94\lambda}{\beta \mathrm{Cos}\theta} \tag{1}$$

where A is the coherence length, β is the full-widths-at-half maximum (FWHM) of the diffraction peak, λ (1.5418 Å) is the wavelength of X-ray radiation, and θ is the angle of diffraction. From different θ values, the calculated average particle size is about 30 nm. Inherent stress inside nanocrystals could contribute to broadening of XRD peaks. The XRD pattern indicates the single phase of Bi_2Te_3 NPs.

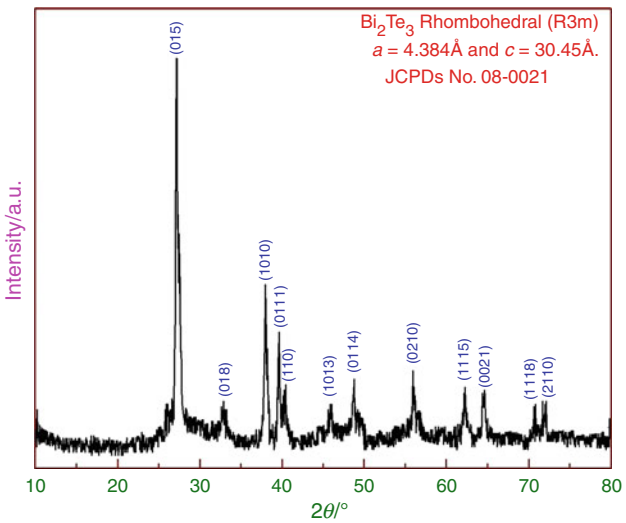

Fig. 1 Room temperature powder XRD pattern of synthesized Bi_2Te_3 NPs

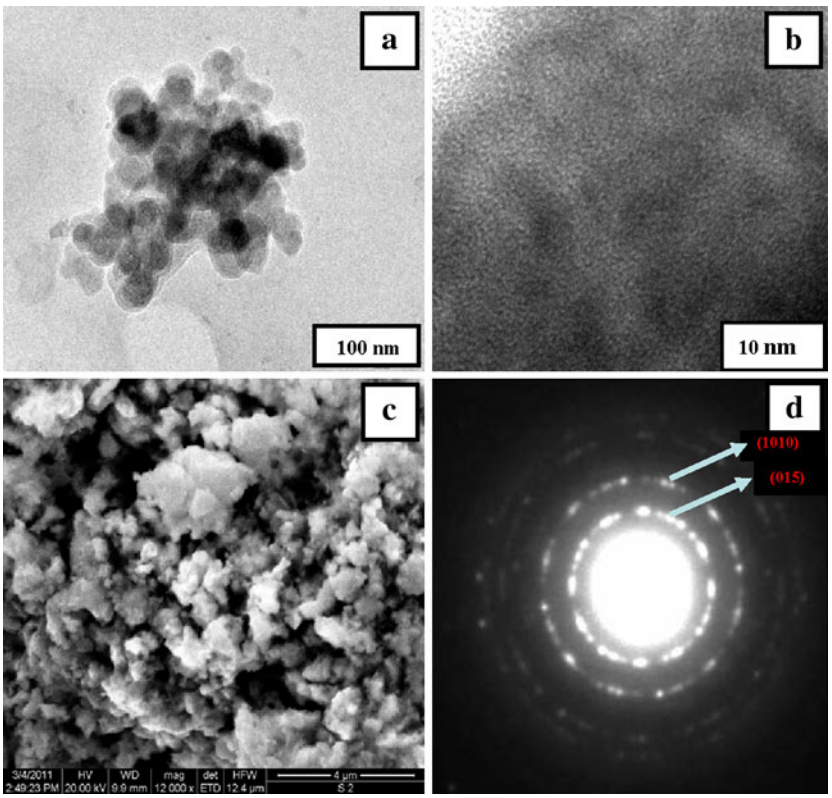

Fig. 2 **a** TEM micrograph, **b** HRTEM micrograph, **c** SEM micrograph and **d** SAED pattern of as synthesized Bi_2Te_3 NPs

The TEM image, shown in Fig. 2a, indicate the high-yield growth feature of the sample synthesized by direct wet chemical route. The HRTEM image of NPs is shown in Fig. 2b, which confirms the crystallinity of the as-synthesized Bi_2Te_3 NPs. On the basis of the TEM and HRTEM images of the NPs, it is revealed that they are agglomerated with the average size of about 30 nm, which is in very good agreement with value obtained from XRD measurement. The morphology of the as-synthesized sample was investigated by SEM. SEM image of as synthesized Bi_2Te_3 NPs is shown in Fig. 2c, which shows that the particles are well agglomerated. Selected area electron diffraction (SAED) pattern of the as-prepared sample is shown in Fig. 2d. This represents the SAED pattern of Bi_2Te_3 with (015) and (1010) diffraction planes. ED pattern shows a set of rings corresponding to the diffraction from different atomic planes of the nanocrystallites.

DSC measurement of Bi_2Te_3 NPs was carried out at the heating rate of 10 °C min^{-1} and in the temperature range from ambient to 502 °C. DSC curve is shown in Fig. 3 This curve shows one endothermic peak, one exothermic peak, and a hump. An endothermic region between 127 °C and 177 °C may be due to the change of NPs from uniform to clustering (collection of nanoparticles), an exothermic region between 227 and 277 °C shows no sharp peak which may be attributed to growth of nanocrystals of Bi_2Te_3, and the hump between 352 and 427 °C may be due to the oxidation of some of the degradation of products and above 427 °C, in the temperature at which our sample becomes melt. DSC profiles show that complete thermal decomposition, dispersion, formation and growth of nanocrystals, and the degradation of the as-synthesized Bi_2Te_3 NPs simultaneously. TG curve of the Bi_2Te_3 NPs was obtained at heating rates of 10 °C min^{-1} as shown in the Fig. 4. Table 1 listed the data on mass losses occurring in the stages of degradation of the NPs in the temperature range 50–700 °C. It can be observed from Table 1 that the thermal behavior and the mass loss of the NPs occurs in three stages: the first, in the range of 50–135 °C (mass loss 18 %), which may be attributed to degradation of Bi_2Te_3 NPs; the second, in the range of 135–407 °C (mass loss 20 %), which may be generally attributed to the evaporation of water and organic components; and third, 700–407 °C (mass loss 10 %), which is related to the degradation of residues. Overall, TG results show a mass loss of 48 % in the as-synthesized Bi_2Te_3 NPs up to 700 °C.

The measurement of thermal conductivity of Bi_2Te_3 NPs was carried out at room temperature by TPS technique. Bi_2Te_3 is a highly anisotropic material due to the difference in strength between weak van der Waals bonds among the adjacent Te atoms and strong covalent bonds between Bi and Te atoms [14]. The thermal conductivity of bulk Bi_2Te_3 is 1.5 W m^{-1} K^{-1} along the cleavage plane (perpendicular to the van der Waals bonding direction), while it reduces to values as low as 0.6 W m^{-1} K^{-1} in the

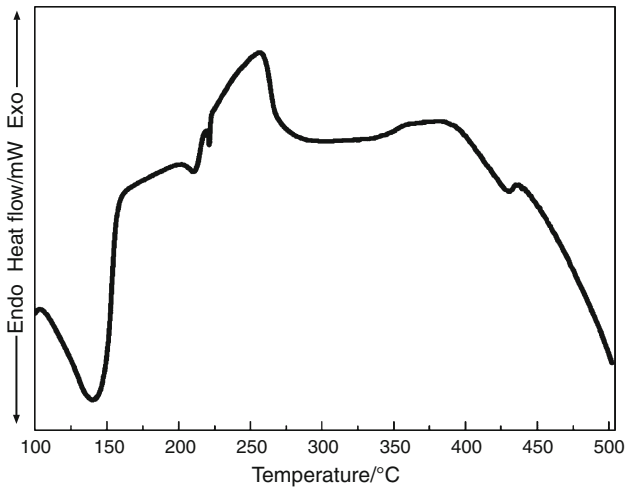

Fig. 3 DSC curve at 10 °C min^{-1} heating rate for Bi_2Te_3 NPs

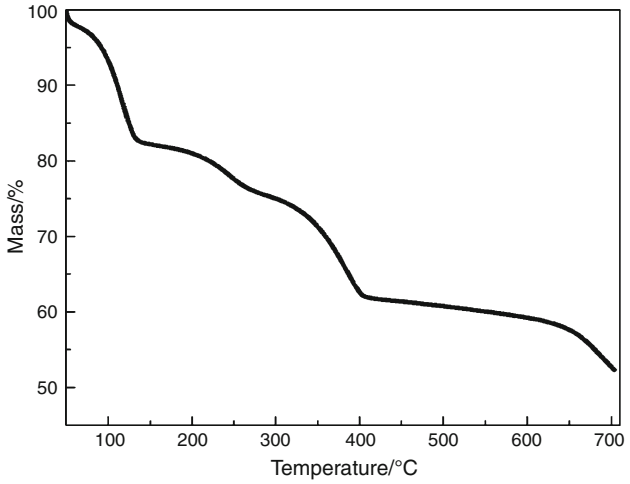

Fig. 4 TG curve of mass as a function of the temperature of as synthesized Bi_2Te_3 NPs

direction perpendicular to the cleavage plane [15]. The low thermal conductivity of Bi_2Te_3 NPs is comparable to that of highly disordered materials. In Bi_2Te_3 NPs, heat conduction proceeds through two types of carriers, phonons, and charge carriers. Goldsmid [16] has investigated mechanisms of heat conduction in Bi_2Te_3 and found that thermal conductivities of the samples with higher doping concentrations were lower than those of samples with reduced doping levels. This effect is attributed to the transport of ionization energy by electron–hole pairs due to the changing carrier concentration in the direction of temperature gradient. Goodson and co-workers [17] have reported that thermal conductivity normal to the Bi_2Te_3/Sb_2Te_3 superlattice layers were found to be about 0.3 W m^{-1} K^{-1}, which is significantly lower than the bulk value for Bi_2Te_3. The obtained thermal conductivity k of the as-synthesized Bi_2Te_3 NPs is about 0.3 W m^{-1} K^{-1} at room temperature. This is a remarkably low value considering the crystalline nature of this material. We also credit this unexpected reduction (as compared to bulk Bi_2Te_3) of the thermal conductivity to the relative importance of low frequency acoustic phonons with longer mean free paths like superlattice layers [17]. It indicates that nanostructuring leads to a remarkable decrease in the thermal conductivity and may be a well-promising result for enhancing the *ZT* value for its use as a good nanomaterials in a thermoelectric device.

Table 1 Data on mass losses occurring in the stages of degradation of the Bi_2Te_3 NPs

Stages	$\Delta T_{experimental}$/°C	Mass loss/%	Attributions
1	135–50 = 85	18	Degradation of Bi_2Te_3
2	407–135 = 272	20	Evaporation of water and organic components
3	700–407 = 293	10	Degradation of residues
Total		48	

Conclusions

In this work, Bi_2Te_3 NPs have been successfully synthesized by low-cost wet chemical route. The Bi_2Te_3 powder obtained at 50 °C consists of agglomerate NPs of average size about 30 nm. The SAED pattern depicted the polycrystalline nature of the as-synthesized nanocrystals, the diffraction ring of which could be indexed to perfect multicrystal diffraction patterns of Bi_2Te_3 NPs. We also studied the thermal effect on the Bi_2Te_3 NPs by DSC and TG curves. TG result shows that only 48 % mass loss has occurred in our product sample. The thermal conductivity of our sample is found to about 0.3 W m^{-1} K^{-1} at room temperature, which is a remarkably low value in revealing the crystallinity nature of the as-synthesized Bi_2Te_3 NPs.

Acknowledgements Punita Srivastava is grateful for the support from CSIR, New Delhi, in providing financial assistance under senior research fellowship (SRF) scheme. We are also thankful to Prof. O. N. Srivastava (Department of Physics, B.H.U.) for XRD, SEM, and TEM measurements and Dr. Pushpendra Kumar (University of Concepcion, Chili) for kind support during the whole course of study.

References

1. Dresselhaus MS, Chen G, Tang MY, Yang RG, Lee H, Wang DZ, Ren ZF, Fleurial JP, Gogna P. New directions for low-dimensional thermoelectric materials. Adv Mater. 2007;19:1043–53.
2. Cao YQ, Zhu TJ, Zhao XB, Zhang XB, Tu JP. Nanostructuring and improved performance of ternary Bi-Sb-Te thermoelectric materials. Appl Phys A Mater Sci Process. 2008;92:321–4.

3. Venkatasubramanian R, Silvola E, Colpitts T, Quinn BO. Thin-film thermoelectric devices with high room-temperature figures of merit. Nature. 2001;413:597–602.
4. Hicks LD, Dresselhaus MS. Effect of quantum-well structures on the thermoelectric figure of merit. Phys Rev B: Condens Matter. 1993;47:16631–4.
5. Hsu KF, Loo S, Guo F, Chen W, Dyck JS, Uher C. Cubic Ag-PbmSbTe^{2+}m: bulk thermoelectric materials with high figure of merit. Science. 2004;303:818–21.
6. Harman TC, Walsh MP, Laforge BE, Turner GW. Nanostructured thermoelectric materials. J Electron Mater. 2005;34:L19–22.
7. Cao YQ, Zhao XB, Zhu TJ, Zhang XB, Tu JP. Syntheses and thermoelectric properties of Bi_2Te_3/Sb_2Te_3 bulk nanocomposites with laminated nanostructure. Appl Phys Lett. 2008;92:143106.
8. Harman TC, Taylor PJ, Walsh MP, LaForge BE. Quantum dot superlattice thermoelectric materials and devices. Science. 2002;297:2229–32.
9. Poudel B, Hao Q, Ma Y, Lan YC, Minnich A, Yu B. High-thermoelectric performance of nanostructured bismuth antimony telluride bulk alloys. Science. 2008;320:634–8.
10. Zhou M, Li JF, Kita T. Nanostructured AgPb(m)SbTe(m^{+2}) system bulk materials with enhanced thermoelectric performance. J Am Chem Soc. 2008;130:4527–32.
11. Mo M, Zeng J, Liu X, Yu W, Zhang S, Qian Y. Controlled hydrothermal synthesis of thin single-crystal tellurium nanobelts and nanotubes. Adv Mater. 2002;14:1658–62.
12. Peng Q, Dong Y, Deng Z, Li Y. Selective synthesis and characterization of CdSe nanorods and fractal nanocrystals. J Inorg Chem. 2002;41:5249–54.
13. Chen YT, Ding JB, Guo Y, Kong LB, Li HL. A facile route to preparation of CdS nanorods. Mater Chem Phys. 2002;77:734–7.
14. Goldsmid HJ. Thermoelectric refrigeration. New York: Plenum; 1964.
15. Touloukian YS, Powell RW, Ho CY, Klemens PG. Thermophysical properties of matter, vol. 1. New York: Plenum; 1970. p. 339.
16. Goldsmid HJ. Heat conduction in bismuth telluride. Proc Phys Soc. 1958;72:17–26.
17. Touzelbaev MN, Zhou P, Venkatasubramanian R, Goodson KE. Thermal characterization of Bi_2Te_3/Sb_2Te_3 superlattices. J Appl Phys. 2001;90(2):763–7.